EurJIC European Journal of Inorganic Chemistry

ChemPubSoc Europe

FULL PAPER

DOI:10.1002/ejic.201300439

Effect of Hydrogen and Oxygen Evolution Cocatalysts on Photocatalytic Activity of GaN:ZnO

CLUSTER ISSUE

Anke Xiong,[a] Taizo Yoshinaga,[b,c] Takahiro Ikeda,[b,c] Masaki Takashima,[d] Takashi Hisatomi,[a] Kazuhiko Maeda,[a,e] Toru Setoyama,[d] Toshiharu Teranishi,[c] and Kazunari Domen*[a]

Keywords: Photochemistry / Photocatalysis / Sustainable chemistry / Nanoparticles / Oxidation / Water splitting / Gallium

The coloading effect of H_2 and O_2 evolution cocatalysts on the overall water splitting reaction was investigated using a solid solution of GaN and ZnO (hereafter termed GaN:ZnO) as a photocatalyst. GaN:ZnO was modified with nanoparticulate Mn_3O_4, RuO_2, and IrO_2 as O_2 evolution cocatalysts and with core/shell-type Rh/Cr_2O_3 composites as H_2 evolution cocatalysts. The photocatalytic activity of the coloaded samples for overall water splitting was higher than that of the samples modified with either of the O_2 or H_2 evolution cocatalysts alone. The activity enhancement induced by coloading was comparable for the three O_2 evolution cocatalysts investigated at the optimized loading amounts. Loading of a more efficient Rh/Cr_2O_3 cocatalyst prepared by adsorption of Rh nanoparticles further improved the photocatalytic activity. It was concluded that a simultaneous improvement in both oxidation and reduction reactions was effective at enhancing the photocatalytic activity of GaN:ZnO, whereas the reduction reactions limited the overall reaction rate of the coloaded system more significantly.

Introduction

Conversion of solar energy into hydrogen energy by photocatalytic water splitting is regarded as a clean and sustainable way to solve worldwide environmental and energy problems.[1–4] Water splitting on a particulate semiconductor photocatalyst involves three steps: i) photoexcitation of electron–hole pairs in the bulk of the photocatalyst, ii) separation and migration of photoexcited carriers to the surface of the photocatalyst, and iii) reduction and oxidization of adsorbed species by photoexcited electrons and holes on the surface of the photocatalyst. In addition, undesirable recombination occurs in parallel to the abovementioned processes. The first step is governed by the light absorption capability of the photocatalyst, whereas the second and the third reactions are influenced by semiconductor qualities (crystallinity, density of defects, mobility of carriers, etc.) and cocatalyst loading, respectively.

The development of narrow band gap semiconductors is needed for the efficient utilization of sunlight. A solid solution of GaN and ZnO (GaN:ZnO) serves as an active photocatalyst for overall water splitting under visible light provided it is modified with the proper cocatalysts.[5–12] Because the GaN:ZnO surface lacks H_2 evolution sites, it is essential to load it with H_2 evolution cocatalysts such as Rh-Cr mixed oxide and core/shell-structured Rh/Cr_2O_3. In addition, it is believed that an improvement in either the reduction or oxidation reaction could increase the overall reaction rate because these reactions proceed on the surface at the same rate in any photocatalytic reaction at steady state. Indeed, it was recently found that coloading of nanoparticulate Mn_3O_4 as an O_2 evolution cocatalyst onto Rh/Cr_2O_3-loaded GaN:ZnO and Pt/Cr_2O_3-loaded $SrTiO_3$ further improved the photocatalytic activity for overall water splitting, though only by a factor of ca. 1.5.[13] In addition, coloading of H_2 and O_2 evolution cocatalysts was also found to be essential for overall water splitting using ZrO_2-modified TaON.[14] Besides cocatalyst loading, calcination treatment of GaN:ZnO was found to reduce the density of zinc- and/or oxygen-related defects, suppressing charge recombination in the photocatalyst, and thus more than doubling the activity for overall water splitting.[15]

The studies above testify to the importance of refining the preparation of the photocatalyst and loading of func-

[a] Department of Chemical System Engineering, The University of Tokyo,
7-3-1 Hongo, Bunkyo-ku, Tokyo 113-8656, Japan
E-mail: domen@chemsys.t.u-tokyo.ac.jp
Homepage: http://www.domen.t.u-tokyo.ac.jp
[b] Graduate School of Pure and Applied Sciences, University of Tsukuba,
1-1-1 Tennodai, Tsukuba, Ibaraki 305-8571, Japan
http://www.chem.tsukuba.ac.jp/teranisi/index_E.html
[c] Institute for Chemical Research, Kyoto University,
Gokasho, Uji, Kyoto,611-0011, Japan
http://www.scl.kyoto-u.ac.jp/~teranisi/index_E.html
[d] Mitsubishi Chemical Group Science and Technology Research Center,
1000 Kamoshida, Aoba, Yokohama 227-8502, Japan
http://www.m-kagaku.co.jp/index_en.htm
[e] Precursory Research for Embryonic Science and Technology (PRESTO), Japan Science and Technology Agency (JST),
4-1-8 Honcho Kawaguchi, Saitama 332-0012, Japan

Supporting information for this article is available on the WWW under http://dx.doi.org/10.1002/ejic.201300439.

tionally designed cocatalysts. However, since cocatalyst coloading and calcination of GaN:ZnO had been studied individually, a detailed investigation into their interrelationship is needed to maximize potential synergistic effects. In the present study, Mn_3O_4 and Rh/Cr_2O_3 were coloaded onto calcined GaN:ZnO as O_2 and H_2 evolution cocatalysts, respectively, in an attempt to combine the positive effects of facilitating surface reactions and enhancing the bulk properties of GaN:ZnO to improve the photocatalytic activity for overall water splitting. In addition, the loading of more efficient cocatalysts was studied to further improve the photocatalytic activity of the coloaded system. Specifically, nanoparticulate RuO_2 and IrO_2 were studied as O_2 evolution cocatalysts since they are known to exhibit better catalytic activity for water oxidation than Mn_3O_4.[16] In the case of the core/shell-type Rh/Cr_2O_3, the Rh core was deposited by adsorption of Rh nanoparticles (NPs),[17,18] which allowed for a better dispersion and higher catalytic activity for water reduction than the conventional photodeposition of Rh.

Results and Discussion

Colloidal suspensions of nanoparticulates of MnO, Ru, and Ir protected with organic ligands were prepared as precursors of Mn_3O_4, RuO_2, and IrO_2 cocatalysts, respectively, according to previously reported methods.[19,20] The particle sizes of MnO, Ru, and Ir were estimated to be 8.8 ± 0.6, 0.9 ± 0.3, and 1.2 ± 0.3 nm, respectively, from the TEM images (Figure S1). These NPs were loaded onto GaN:ZnO before and after calcination at 873 K [represented as GaN:ZnO(a) and GaN:ZnO(c), respectively] by adsorption or impregnation, being converted into the desired oxygen evolution cocatalysts upon calcination at 673 K to eliminate organic protecting ligands (Figure S2). Subsequently, Rh/Cr_2O_3 were loaded onto GaN:ZnO modified with O_2 evolution cocatalysts by a previously reported sequential photodeposition method.[13]

TEM images of GaN:ZnO(a) and GaN:ZnO(c) modified with Mn_3O_4 alone and both Cr_2O_3/Rh and Mn_3O_4 revealed that the size of manganese oxide NPs was unchanged by the loading of Rh/Cr_2O_3 using photodeposition (Figure 1). Rh/Cr_2O_3 was characterized by a Cr_2O_3 shell in a lighter colour than a Rh core whereas Mn_3O_4 was not. This is because Cr_2O_3 was photodeposited from Cr^{6+} ions only on reduction sites whereas Rh was loaded on the photocatalyst.[12] TEM-EDX analysis also confirmed that the Rh/Cr_2O_3 and Mn_3O_4 NPs were loaded separately on the photocatalysts. Thus, possible changes in the surface properties of GaN:ZnO because of the post-calcination treatment did not have a significant effect on the loading conditions of the Mn_3O_4 oxygen evolution cocatalyst. Separate loading of H_2 and O_2 evolution cocatalysts was also suggested for IrO_2 (Figure S1). IrO_2 loaded NPs were barely observable because of the small particle size. However, IrO_2 NPs could be distinguished from Rh/Cr_2O_3 by comparing the particle sizes. On the other hand, the particle size of RuO_2 was too small to observe by TEM. However, the presence of the Ru species was confirmed by EDX analysis and the photocatalytic activity was indeed improved by coloading of RuO_2. These observations suggest that RuO_2 was deposited separately from Rh/Cr_2O_3 without deteriorating the performance. It is presumed that Rh/Cr_2O_3 did not coat the O_2 evolution cocatalysts because Rh/Cr_2O_3 was deposited on the reduction sites of the photocatalyst surface by photodeposition. In fact, the Mn_3O_4 and IrO_2 NPs were free of Rh/Cr_2O_3 core/shell-type composites. On the other hand, Rh/Cr_2O_3 NPs could be deposited onto RuO_2 since they served as both reduction and oxidation sites on GaN:ZnO. However, it was confirmed that GaN:ZnO(c) loaded with 0.05 wt.-% RuO_2 showed no activity for the sacrificial H_2 evolution reaction from aqueous methanol (10 vol.-%) under visible light irradiation. This suggests that the loaded RuO_2 functions as an O_2 evolution cocatalyst when coloaded with Rh/Cr_2O_3, which is more efficient as an H_2 evolution cocatalyst.

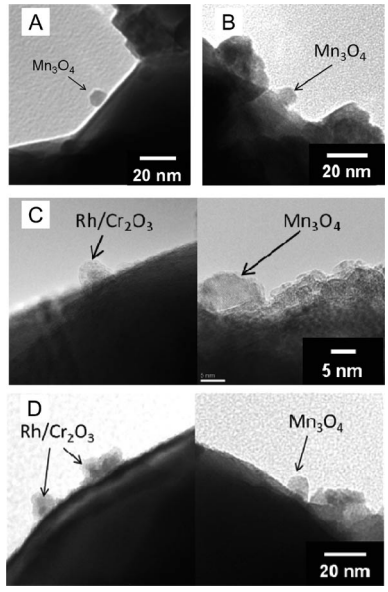

Figure 1. TEM images of (A) Mn_3O_4/GaN:ZnO(a), (B) Mn_3O_4/GaN:ZnO(c), (C) Cr_2O_3/Rh-Mn_3O_4/GaN:ZnO(a), and (D) Cr_2O_3/Rh-Mn_3O_4/GaN:ZnO(c).

As shown in Figure 2, the photocatalytic activity of GaN:ZnO(c) modified with Mn_3O_4 and Rh/Cr_2O_3 was greater than that of the sample loaded with only Rh/Cr_2O_3 when the loading amount of Mn_3O_4 was relatively low (ca. 0.05 wt.-%). GaN:ZnO(c) modified with Mn_3O_4 alone showed no activity for overall water splitting. These results parallel those of as-prepared GaN:ZnO. GaN:ZnO(c) coloaded with Mn_3O_4 and Rh/Cr_2O_3 showing highest activity at 0.02 wt.-% of Mn_3O_4 NP loading. The photocatalytic activity of Rh/Cr_2O_3-loaded GaN:ZnO subjected to calcination prior to cocatalyst loading and/or loading of the Mn_3O_4 cocatalyst before photodeposition of Rh/Cr_2O_3 is depicted in Figure 3. This graphic (Figure 3) permits better comparison of the effects of these procedures. The photocatalytic activity of Rh/Cr_2O_3-loaded GaN:ZnO (Figure 3,

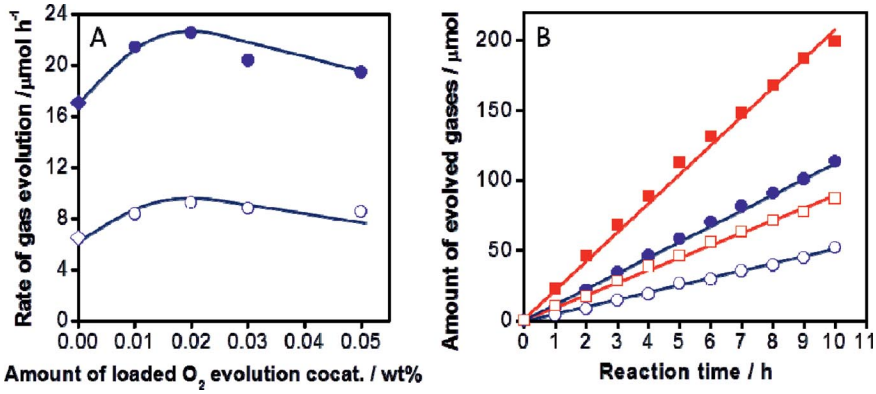

Figure 2. (A) Dependence of the photocatalytic activity of Cr_2O_3/Rh-loaded GaN:ZnO(c) for overall water splitting on the loading amount of Mn_3O_4. (B) Time course of overall water splitting using GaN:ZnO coloaded with Cr_2O_3/Rh and Mn_3O_4. Reaction conditions: catalyst, 0.1 g; solution, H_2O 100 mL; light source, 300 W Xe lamp with a cutoff filter ($\lambda > 420$ nm); reaction vessel, Pyrex top-irradiation vessel. Rectangles and circles represent GaN:ZnO(c) and GaN:ZnO(a), respectively. Closed and open symbols denote H_2 and O_2, respectively.

C) was improved by factors of 2.3, 1.5, and 3.4, respectively, through calcination of GaN:ZnO (Figure 3, D), coloading of Mn_3O_4 (Figure 3, E), and a combination of these two treatments (Figure 3, F). Clearly, the effects of calcining GaN:ZnO and coloading Mn_3O_4 were accumulative. Previous studies have concluded that calcination of GaN:ZnO reduced defect densities and suppressed recombination of photoexcited holes and electrons in the bulk and that coloading of Mn_3O_4 facilitated water oxidation on the surface. These results suggest that improvements to the bulk properties of the photocatalyst and the surface reaction kinetics independently enhance the activity of the photocatalyst for overall water splitting. It should be noted that the loading amounts of the O_2 evolution cocatalyst were significantly lower than that of the H_2 evolution cocatalyst. This is probably because GaN:ZnO was inactive for H_2 evolution reactions without the aid of H_2 evolution cocatalysts, whereas it was active for O_2 evolution reactions even in the absence of O_2 evolution cocatalysts.

The photocatalytic activity of GaN:ZnO(c) modified with different O_2 evolution cocatalysts and Rh/Cr_2O_3 for overall water splitting is summarized in Figure 4. All O_2 evolution cocatalysts examined in this work improved the activity compared to the sample loaded with Rh/Cr_2O_3 alone. The optimal amount of O_2 evolution cocatalyst was almost always the same (0.02–0.03 wt.-%) regardless of its identity. Such quantities of O_2 evolution cocatalyst are very small relative to H_2 evolution cocatalyst Rh (0.75 wt.-%). A similar result was obtained for O_2 evolution reactions from an aqueous $NaIO_3$ solution using WO_3 coloaded with Pt and RuO_2 as reduction and oxidation cocatalysts, respectively,[21] where the loading amount of RuO_2 (0.001 wt.-%) was much smaller than that of Pt (0.5 wt.-%). Another important observation was that the photocatalytic activity of GaN:ZnO(c) coloaded with the O_2 and H_2 evolution cocatalysts was almost the same regardless of the kind of O_2 evolution cocatalyst used at respective optimal loadings. This suggests that reduction, rather than oxidation reac-

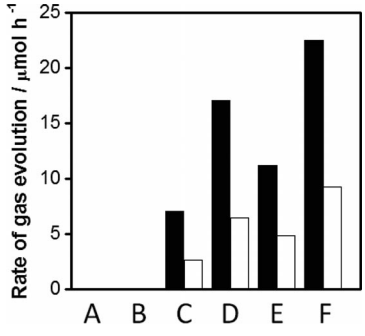

Figure 3. Photocatalytic activity of (A) Mn_3O_4/GaN:ZnO(a), (B) Mn_3O_4/GaN:ZnO(c), (C) Cr_2O_3/Rh/GaN:ZnO(a), (D) Cr_2O_3/Rh/GaN:ZnO(c), (E) Cr_2O_3/Rh-Mn_3O_4/GaN:ZnO(a), and (F) Cr_2O_3/Rh-Mn_3O_4/GaN:ZnO(c) for overall water splitting. Reaction conditions: catalyst, 0.1 g; solution, H_2O 100 mL; light source, 300 W Xe lamp with a cutoff filter ($\lambda > 420$ nm); reaction vessel, Pyrex top-irradiation vessel. Black and white bars indicate H_2 and O_2 evolution rates, respectively.

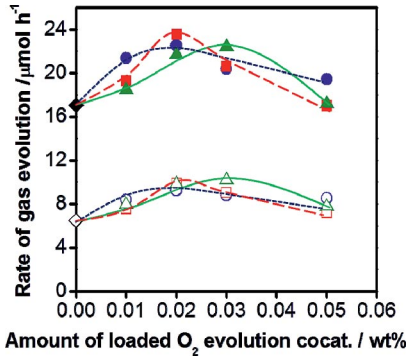

Figure 4. The photocatalytic activity of GaN:ZnO(c) coloaded with different O_2 evolution cocatalysts and Rh/Cr_2O_3. Reaction conditions: catalyst, 0.1 g; solution, H_2O 100 mL; light source, 300 W Xe lamp with a cutoff filter ($\lambda > 420$ nm); reaction vessel, Pyrex top-irradiation vessel. Circles, triangles, and squares indicate the loading of Mn_3O_4, IrO_2, and RuO_2, respectively. Closed and open symbols denote H_2 and O_2, respectively.

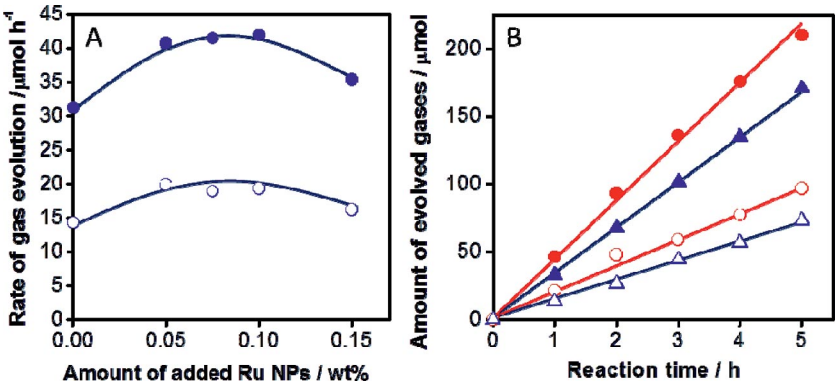

Figure 5. (A) Dependence of the photocatalytic activity of GaN:ZnO(c) loaded with Cr_2O_3/Rh by adsorption of Rh NPs on the loading amount of RuO_2. (B) Time course of overall water splitting using GaN:ZnO(c) coloaded with RuO_2 and Cr_2O_3/Rh prepared by adsorption of Rh NPs (circles) and photodeposition of Rh (triangles). Reaction conditions: catalyst, 0.1 g; solution, H_2SO_4 aq. 100 mL (pH 4.5); light source, 300 W Xe lamp with a cutoff filter ($\lambda > 420$ nm); reaction vessel, Pyrex top-irradiation vessel.

tions, play the dominant role in limiting the net activity of GaN:ZnO for overall water splitting.

To determine the impact of H_2 evolution cocatalyst on the coloaded system, a more efficient Rh/Cr_2O_3 prepared from nanoparticulate Rh was employed. The use of nanoparticulate Rh prevented the aggregation of Rh cores often observed in the photodeposition of Rh[12] and thus improved the activity of the H_2 evolution cocatalyst. Rh NPs 3.3 ± 0.8 nm in size (Figure S3) were prepared by the same method as Ru NPs except that $RhCl_3$ was used instead of $RuCl_3$. NPs of Ru and Rh were sequentially adsorbed onto GaN:ZnO(c). After removal of the organic ligands by calcination, the Cr_2O_3 shell was deposited onto the sample by the photodeposition method. Notably, the calcination process caused partial oxidation of the Rh core, in addition to conversion of Ru into RuO_2 NPs, although the partially oxidized Rh core catalyzed H_2 evolution just as efficiently as the conventional Rh core, deposited by photodeposition.[17,18] The core/shell structure characteristic of Rh/Cr_2O_3 was confirmed by TEM observation, whereas the RuO_2 NPs could not be identified because of their small size (Figure S3), similar to the case of the photodeposition method.

As shown in Figure 5, the coloading effect of H_2 and O_2 evolution cocatalysts was confirmed when Rh/Cr_2O_3 was prepared by adsorption of Rh NPs. The optimal amount of RuO_2 NPs was approximately 0.05–0.1 wt.-%. The sample modified with Rh cores by adsorption showed a higher activity for overall water splitting than the sample loaded with Rh cores by photodeposition. In the case of the Rh/Cr_2O_3 cocatalyst prepared by the photodeposition method, facilitating O_2 evolution kinetics by increasing the loading amount of the O_2 evolution cocatalyst did not lead to further improvement in the photocatalytic activity, as shown in Figure 4. However, enhancing H_2 evolution kinetics by applying Rh NPs did indeed improve the overall photocatalytic activity. These results indicate that the rate of H_2 evolution limited the net activity of GaN:ZnO for water splitting. It seems that the optimal loading amount of RuO_2 was slightly higher when the Rh core of Rh/Cr_2O_3 was deposited by adsorption of Rh NPs instead of photodeposition. This is possibly because reduction and oxidation reaction rates need to be balanced in photocatalytic reactions. As the activity of H_2 evolution cocatalysts improve, photocatalysts will need to accommodate larger amounts of O_2 evolution cocatalysts or more efficient O_2 evolution cocatalysts to balance the rates of reduction and oxidation chemistries.

Conclusions

Coloading of Mn_3O_4, RuO_2, and IrO_2 NPs as O_2 evolution cocatalysts increased the photocatalytic activity of GaN:ZnO modified with Rh/Cr_2O_3 as an H_2 evolution cocatalyst. Accumulative positive effects were obtained by coloading of the O_2 evolution cocatalysts to facilitate surface O_2 evolution kinetics and annealing of the photocatalyst to improve bulk properties. The optimal loading amounts of the O_2 evolution cocatalysts were much lower than those of the H_2 evolution cocatalysts. In addition, the photocatalytic activity for overall water splitting was largely independent of the kind of O_2 evolution cocatalyst. On the other hand, applying a more efficient H_2 evolution cocatalyst prepared by adsorption of Rh NPs improved the photocatalytic activity of the coloaded system. These results indicate that the activity of GaN:ZnO was more strongly limited by H_2 evolution reactions, although coloading of O_2 evolution cocatalysts improved the photocatalytic performance to some extent. In this way, a deeper understanding of the bulk properties of the photocatalyst and kinetic enhancement by cocatalysts can offer more rational designs for photocatalytic systems.

Experimental Section

Synthesis of GaN:ZnO Photocatalyst: A GaN:ZnO solid solution was prepared according to a previously reported method.[5] Briefly, a mixture of Ga_2O_3 (1.08 g) and ZnO (0.94 g) powders was heated at 1098 K under flowing NH_3 (250 mL min^{-1}) for 13 h. After nitrid-

ation, the sample was cooled to room temperature, maintaining the NH_3 flow throughout. Calcination treatment was carried out by heating the obtained sample at 873 K in air for 5 h. The production of GaN:ZnO with the composition Zn/Ga ≈ 0.13 was confirmed by powder X-ray diffraction and energy-dispersive X-ray analysis. The band gap energy of the prepared GaN:ZnO was 2.68 eV, as estimated from the onset of the diffuse reflectance spectrum. The BET specific surface area of the sample was 9.4 $m^2 g^{-1}$. These physical properties were nearly unaffected by the post-calcination treatment.

Synthesis of MnO Nanoparticles: MnO nanoparticles were synthesized according to a procedure similar to the technique reported in the literature.[19] The procedure involved the preparation of Mn oleate, followed by heating in 1-octadecene. Mn oleate was prepared by reacting $Mn(NO_3)_2{\cdot}6H_2O$ (40 mmol) and sodium oleate (80 mmol) in a mixed solvent of ethanol (30 mL), distilled water (40 mL), and hexane (70 mL) at 343 K under N_2 overnight. The solution was then transferred to a separatory funnel, and the upper organic layer was collected. After evaporation of the organic solvent, a pink colored Mn oleate was obtained. The crude Mn oleate (0.25 g, 0.4 mmol) was heated in 1-octadecene (10 mL) according to the following procedure: The mixture was heated at 393 K for 1 h under vacuum. Then, the temperature was increased at a rate of 10 K min^{-1} to 573 K under nitrogen atmosphere. After the mixture was stirred magnetically at 573 K for 30 min, the temperature was slowly lowered to room temperature in the mantle heater. A mixed solution of methanol and ethyl acetate was added to the crude product, and the mixture was purified by centrifugation. Finally, the precipitate was redispersed in THF (20 mL).

Loading Mn_3O_4 Nanoparticles Onto GaN:ZnO: Mn_3O_4 nanoparticles were loaded onto GaN:ZnO according to a procedure reported in the literature.[13] GaN:ZnO (170 mg) powder was suspended in THF (total 16 mL) containing the desired amount of MnO nanoparticles. After ultrasonication, a THF solution (5 mL) of 16-hydroxyhexadecanoic acid (20 mmol) was added to the suspension, which was then stirred for 3 h. After stirring, the MnO-containing GaN:ZnO was washed with THF and hexane by centrifugation, and then heated in air at 673 K for 3 h (ramp: 5 K min^{-1}) to remove organic residues. This calcination procedure converted the NaCl-type MnO into spinel-type Mn_3O_4, but the particle size of the manganese oxide remained unchanged.

Synthesis of Ru, Ir, and Rh Nanoparticles: The suspensions of nanoparticulate Ru, Ir, and Rh were prepared by an alcohol-reduction method reported by N. Toshima et al.[20] An aqueous 50 vol.-% EtOH solution (50 mL) containing 1 mmol L^{-1} metal ions ($RuCl_3$ or Na_2IrCl_6 or $RhCl_3$) and 40 mmol L^{-1} PVP as a protective ligand was stirred and refluxed by heating at 373 K for 2 h. The resultant colloidal dispersion was purified by acetyl acetate, and re-dispersed in an aqueous 50 vol.-% EtOH solution (50 mL).

Loading RuO_2 and IrO_2 Nanoparticles Onto GaN:ZnO: Nanoparticulate RuO_2 and IrO_2 as O_2 evolution cocatalysts were loaded onto GaN:ZnO(c) by a wet impregnation method. Briefly, GaN:ZnO(c) powder (0.13 g) and distilled water (3–4 mL) containing an appropriate amount of Ru or Ir colloidal dispersion were placed in an evaporating dish on a water bath. The suspension was stirred by a glass rod until complete evaporation. The dried powder was collected and heated in air at 673 K for 2 h to remove PVP and simultaneously oxidize the loaded metallic nanoparticles to relative oxides.

Loading Rh/Cr_2O_3 (Core/Shell) Nanoparticles Onto O_2 Evolution Cocatalyst-loaded GaN:ZnO: Core/shell-type Rh/Cr_2O_3 composites, serving as H_2 evolution cocatalyst, were loaded on the photocatalysts by an in situ photodeposition method detailed in a previous report.[12] The O_2 evolution cocatalyst-loaded sample (0.13 g) was dispersed in aqueous Na_3RhCl_6 solution (0.17 mM). After irradiation by visible light ($\lambda > 420$ nm) using a 300 W Xe lamp with a cutoff filter for 4 h, the Rh^{III} species were reduced into metallic Rh under air-free conditions. Then, K_2CrO_4 (0.8 mM) was added to the solution, which was subjected to further visible irradiation ($\lambda > 420$ nm) for another 4 h to reduce K_2CrO_4 to Cr_2O_3. The loading amounts of Rh and Cr used in this procedure were ≈ 0.75 and 0.31 wt.-%, respectively. The temperature of the reactant solution was maintained at room temperature by a flow of cooling water during the whole process. The samples obtained were washed well with distilled water and dried overnight at 343 K.

Coloading RuO_2 and Rh/Cr_2O_3 Nanoparticles Onto GaN:ZnO Using Rh NPs as a Core: Nanoparticulate RuO_2 as an O_2 evolution cocatalyst and nanoparticulate Rh as a H_2 evolution cocatalyst were coloaded onto GaN:ZnO(c) by adsorbing Ru and Rh NPs step by step. Briefly, GaN:ZnO(c) powder (0.13 g) was suspended in an aqueous 50 vol.-% EtOH solution (20 mL) containing the appropriate amount of Ru NPs. After 2 h of stirring, a Rh colloidal dispersion (1.0 wt.-% Rh loading) was added to the suspension, which was stirred for another 3 h. After filtration and drying at 343 K overnight, the Ru and Rh NP coloaded GaN:ZnO(c) was heated in air at 673 K for 2 h. Finally, the sample was loaded with Cr_2O_3 shells by the photodeposition method described above.

Photocatalytic Reactions: The photocatalytic water splitting reactions were carried out using the same experimental setup as that used for the photodeposition of Rh/Cr_2O_3 on photocatalysts. The prepared sample (0.1 g) was suspended in H_2O or aqueous H_2SO_4 (pH 4.5) (100 mL), followed by evacuation of air from the reaction solution. Irradiation was conducted using a 300 W Xe lamp with an L-42 cutoff filter. The evolved gases were analyzed by gas chromatography (Shimadzu, GC-8A with TCD detector and MS-5A column, argon carrier gas).

Supporting Information (see footnote on the first page of this article): TEM images and XRD patterns of the cocatalysts.

Acknowledgments

This work was supported in part by the Japan Society for the Promotion of Science (JSPS) through a grant-in-Aid for Specially Promoted Research (#23000009) and by Japan Science and Technology Agency (JST) through the Advanced Low Carbon Technology Research and Development Program (ALCA). This work was partly supported by the Cabinet Office of Japan through the Funding Program for World-Leading Innovative R&D in Science and Technology (FIRST). This work also contributes to the international exchange program of the A3 Foresight Program of JSPS. One of the authors (A. X.) was supported by Japan Chemical Industry Association. K. M. thanks the Nippon Sheet Glass Foundation for Materials Science and Engineering for funding support. Acknowledgments are also extended to the Japan Society for the Promotion of Science KAKENHI (grant 23245028, to T. T.) and the Japan Society for the Promotion of Science, Research Fellowship for Young Scientists (grant 24.2251, to T. Y.).

[1] J. S. Lee, *Catalysts. Catal. Surv. Asia* **2005**, *9*, 217.
[2] K. Maeda, K. Domen, *J. Phys. Chem. C* **2007**, *111*, 7851.
[3] F. E. Osterloh, *Chem. Mater.* **2008**, *20*, 35.
[4] A. Kudo, Y. Miseki, *Chem. Soc. Rev.* **2009**, *38*, 253.
[5] K. Maeda, T. Takata, M. Hara, N. Saito, Y. Inoue, H. Kobayashi, K. Domen, *J. Am. Chem. Soc.* **2005**, *127*, 8286.

[6] K. Maeda, K. Teramura, T. Takata, M. Hara, N. Saito, K. Toda, Y. Inoue, H. Kobayashi, K. Domen, *J. Phys. Chem. B* **2005**, *109*, 20504.
[7] K. Teramura, K. Maeda, T. Saito, T. Takata, N. Saito, Y. Inoue, K. Domen, *J. Phys. Chem. B* **2005**, *109*, 21915.
[8] K. Maeda, K. Teramura, D. Lu, T. Takata, N. Saito, Y. Inoue, K. Domen, *Nature* **2006**, *440*, 295.
[9] K. Maeda, K. Teramura, H. Masuda, T. Takata, N. Saito, Y. Inoue, K. Domen, *J. Phys. Chem. B* **2006**, *110*, 13107.
[10] K. Maeda, K. Teramura, D. Lu, T. Takata, N. Saito, Y. Inoue, K. Domen, *J. Phys. Chem. B* **2006**, *110*, 13753.
[11] K. Maeda, K. Teramura, N. Saito, Y. Inoue, K. Domen, *J. Catal.* **2006**, *243*, 303.
[12] K. Maeda, K. Teramura, D. Lu, N. Saito, Y. Inoue, K. Domen, *Angew. Chem.* **2006**, *118*, 7970; *Angew. Chem. Int. Ed.* **2006**, *45*, 7806.
[13] K. Maeda, A. Xiong, T. Yoshinaga, T. Ikeda, N. Sakamoto, T. Hisatomi, M. Takashima, D. Lu, M. Kanehara, T. Setoyama, T. Teranishi, K. Domen, *Angew. Chem.* **2010**, *122*, 4190; *Angew. Chem. Int. Ed.* **2010**, *49*, 4096.
[14] K. Maeda, D. Lu, K. Domen, *Chem. Eur. J.* **2013**, *19*, 4986.
[15] K. Maeda, K. Teramura, K. Domen, *J. Catal.* **2008**, *254*, 198.
[16] A. Harriman, I. J. Pickering, J. M. Thomas, P. A. Christensen, *J. Chem. Soc. Faraday Trans. 1* **1988**, *84*, 2795.
[17] N. Sakamoto, H. Ohtsuka, T. Ikeda, K. Maeda, D. Lu, M. Kanehara, K. Teramura, T. Teranishi, K. Domen, *Nanoscale* **2009**, *1*, 106.
[18] T. Ikeda, A. Xiong, T. Yoshinaga, K. Maeda, K. Domen, T. Teranishi, *J. Phys. Chem. C* **2013**, *117*, 2467.
[19] H. B. Na, J. H. Lee, K. An, Y. I. Park, M. Park, I. S. Lee, D.-H. Nam, S. T. Kim, S.-H. Kim, S.-W. Kim, K.-H. Lim, K.-S. Kim, S.-O. Kim, T. Hyeon, *Angew. Chem.* **2007**, *119*, 5493; *Angew. Chem. Int. Ed.* **2007**, *46*, 5397.
[20] N. Toshima, Y. Yamaji, T. Teranishi, T. Yonezawa, *Z. Naturforsch. A* **1995**, *50*, 283.
[21] S. S. K. Ma, K. Maeda, R. Abe, K. Domen, *Energy Environ. Sci.* **2012**, *5*, 8390.

Received: April 3, 2013
Published Online: July 16, 2013

